The role of temperature on the structure and dimensionality of MOFs: an illustrative study of the formation of manganese oxy-bis(benzoate) structures†

Partha Mahata,[a] A. Sundaresan[b] and Srinivasan Natarajan*[a]

Received (in Cambridge, UK) 30th May 2007, Accepted 8th August 2007
First published as an Advance Article on the web 20th August 2007
DOI: 10.1039/b708060c

Three new manganese oxy-bis(benzoate) compounds, synthesized by increasing the reaction temperature, with increasing dimensionality and decreasing Mn–Mn distances, indicate a possible pathway through an entropy driven dehydration route.

One of the emerging trends in the area of metal–organic frameworks (MOF) appears to be the study of the possible competition between the thermodynamic and the kinetic factors in the formation of such structures.[1] Recent studies indicate that, in few cases, the thermodynamic considerations outweigh the kinetic ones. Cheetham and co-workers provided the first insight towards this aspect during their study on the formation of cobalt succinate phases,[2] which showed that denser higher dimensional structures are formed on increasing the reaction temperature through an entropy driven dehydration pathway. A similar trend has also been observed in the formation of nickel diphosphonate, $[Ni_4(O_3P(CH_2)PO_3)_2{\cdot}n(H_2O)$ (n = 3, 2, 0)],[3] and the cobalt pyridine-3,4-dicarboxylates, $[Co(3,4\text{-pyda})(H_2O)_2]{\cdot}H_2O$ and $[Co_3(OH)_2(3,4\text{-pyda})_2(H_2O)_2]$.[4] We, therefore, considered it important to investigate the formation of MOF structures, in which synthesis temperature is the only variable. For this study, we investigated the formation of manganese 4,4′-oxy bis(benzoate) (OBA) compounds by varying the reaction temperature. The compounds, $[\{Mn(H_2O)_3\}\{C_{12}H_8O(COO)_2\}]{\cdot}H_2O$, **I**, $[\{Mn(H_2O)\}\{C_{12}H_8O(COO)_2\}]$, **II**, and $[\{Mn(OH)\}_2\{C_{12}H_8O\text{-}(COO)_2\}]$, **III**, have been prepared as pure phases at three different temperatures, 100, 160 and 220 °C, respectively.‡

The octahedral Mn^{+2} ions in **I** were coordinated by three water molecules and three carboxylate oxygens, where the two carboxylate groups of the OBA anion show both bis-monodentate and monodentate connectivity with the Mn^{+2} ions. The connectivity between the carboxylate groups and $Mn(H_2O)_3O_3$ octahedra gives rise to one-dimensional wire-like structures, which are connected by the OBA unit, forming a two-dimensional layer structure (Fig. 1a).

The square pyramidal Mn^{+2} ions in **II** are coordinated by one water molecule and four carboxylate oxygen atoms, where the carboxylate group of the OBA anion has bis-monodentate connectivity with the Mn^{+2} ions. The central oxygen atoms [O(4)] of the OBA anions lie on a two-fold axis. The Mn^{2+} ions are linked to the carboxylate units, forming 8-membered rings, which are connected through their corners, forming a one-dimensional chain. The eight-membered ring $[Mn_2O_4C_2]$ lies about an inversion centre. The chains are bonded with the OBA units, forming the two-dimensional layer structure (Fig. 1b). The structure of **II** is similar to the structures of $[M(H_2O)(OBA)]$, M = Zn, Cd, reported previously.[5]

The Mn^{+2} ions in **III** are octahedrally coordinated by the carboxylate oxygens, O(2), O(3) and O(1) (–OH). The two oxygen atoms of the OBA anion have bis-monodentate [O(3)] and monodentate [O(2)] connectivity with the Mn^{+2} ions. The central oxygen atoms [O(4)] of the OBA anions lie on a mirror plane. Three Mn^{+2} ions are connected by an –OH [O(1)] group forming a $[Mn_3(\mu_3\text{-OH})]$ triangular unit. Similar units are also known with Co^{+2} ions.[6] The overall two-dimensional layer is formed by the connectivity of the $[Mn_3(\mu_3\text{-OH})]$ triangular unit and the carboxylate oxygens (Fig. 1c). This layer closely resembles the brucite layer (replacing half the –OH ions from the brucite by the carboxylate oxygen; see ESI†). The MnO_6 octahedra are connected with five similar MnO_6 units, of which three are edge-shared and two are corner-shared (Fig. 1c). In brucite the connectivities between the MnO_6 octahedra are identical and all the vertices are –OH groups, resulting in a near perfect hexagon. In **III**, however, half the –OH groups are replaced by carboxylate oxygens, giving rise to differences and distortions in the connectivity within the layer. The inorganic layers are connected by the OBA unit to form the three-dimensional structure (Fig. 1d).

The most noticeable aspect of the present structures, **I–III**, is the degree of dehydration. Some of the aqua molecules were either removed or deprotonated at higher temperatures to give hydroxide groups, which is the key to the formation of **III**. To understand the formation of the different phases, the same reaction mixture was subjected to different temperatures in the range 80–220 °C in steps of 20 °C for 24 h each. The powder XRD patterns of the products of these reactions are shown in Fig. 2. As can be noted, at 80 °C, an unidentified phase is present in addition to **I**. At all other temperatures we observed only the phases (pure or a mixture) discovered in the present study. The formation of a denser 3D structure at higher temperature also gives rise to higher coordinating OBA anions with the metal centres (3 in **I**, 4 in **II** and 6 in **III**). Simultaneously, the Mn–Mn distances are also shortened (4.85 Å in **I**, 4.36 Å in **II** and 3.2 Å in **III**). The isolation of a highly hydrated pseudo two-dimensional structure at low temperature and a fully dehydrated metal oxide/hydroxide

[a]*Framework Solids Laboratory, Solid State and Structural Chemistry Unit, Indian Institute of Science, Bangalore 560 012, India. E-mail: snatarajan@sscu.iisc.ernet.in; Fax: +91-80-2360-1310*
[b]*Chemistry and Physics of Material Unit, Jawaharlal Nehru Centre For Advanced Scientific Research, Bangalore 560 064, India*
† Electronic supplementary information (ESI) available: X-Ray crystallographic data, XRD pattern, IR, EPR, TGA, magnetic studies and additional figures. See DOI: 10.1039/b708060c

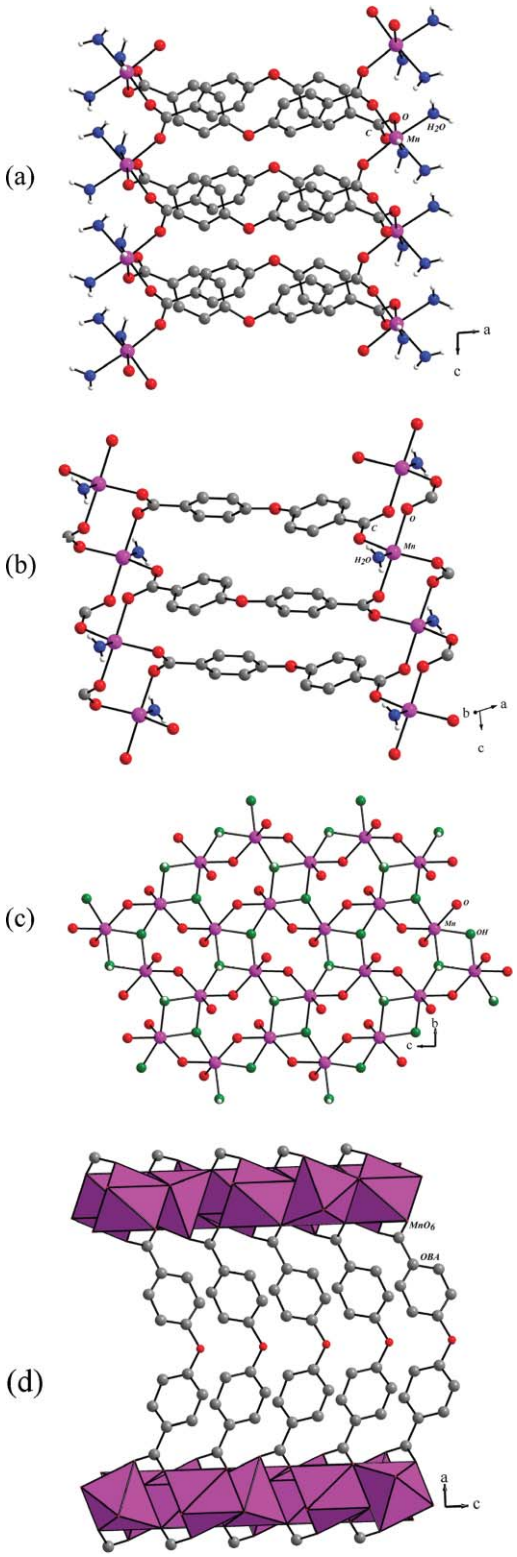

Fig. 1 (a) Structure of **I** in the *ac* plane; (b) the two-dimensional structure of **II**; (c) view of the two-dimensional layer of **III**; (d) connectivity between the two layers by OBA units in **III**.

structure at higher temperature, clearly show that the formation of the framework is influenced by classical thermodynamic factors, such as condensation due to entropy driven dehydration reaction at higher temperature. Transformation reactions have been studied

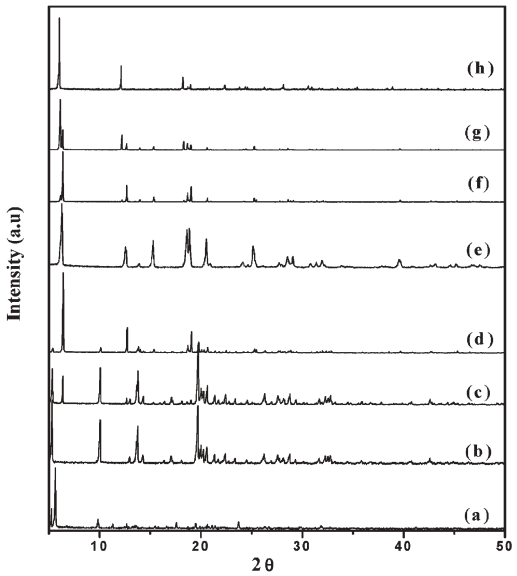

Fig. 2 Powder XRD patterns of the products obtained at different temperatures: (a) 80 (**I** and unknown phase); (b) 100 (pure **I**); (c) 120 (**I** and **II**); (d) 140 (**I** and **II**); (e) 160 (pure **II**); (f) 180 (**II** and **III**); (g) 200 (**II** and **III**); (h) 220 (pure **III**) in °C.

extensively by modifying reaction conditions,[7] but to our knowledge this is the first attempt in MOFs of aromatic carboxylates where the temperature effects have been investigated and correlated with the structure.

We sought to investigate the transformations between the three phases, independently, by carrying out reactions in the solid state as well as employing solution routes (hydrothermal). The studies show that **I** transforms completely to **II**, when heated in the presence of water at 160 °C in an autoclave. **I** transforms to a partially crystalline phase that appears to be related to **II** in 8 h, and becomes poorly crystalline with no resemblance to **II** after 24 h when heated directly at 160 °C in air in the solid state (see ESI†). Similar reactions at 220 °C with **II** did not produce **III**, in either of the reaction conditions (see ESI†). It is likely that the transformation of **I** to **II** goes through the solution-mediated route *via* a simple dehydration process, while both the dehydration and the deprotonation processes are required to form **III**.

The presence of a classical spin ion (Mn^{+2}, $S = 5/2$) in **I–III** prompted us to investigate the magnetic behavior in the temperature range 2–300 K using a SQUID magnetometer. Both the compounds **I** and **II** show simple antiferromagnetic behavior (see ESI†).

Due to the presence of Mn–O–Mn bonds and much smaller Mn–Mn distances, the magnetic behavior of **III** is expected to show considerable difference compared to **I** and **II** (Fig. 3a). As can be noted, the χ_M value increases steadily upon cooling to reach a maximum at $T \sim 40$ K, indicative of the onset of long-range magnetic ordering. The χ_M value decreases upon cooling further up to 8 K, beyond which it again increases. The $1/\chi_M$ *vs.* T curve is shown as the inset of Fig. 3a. The high temperature magnetic susceptibility data (100–300 K) fitted to the Curie–Weiss behavior with $C = 4.37$ emu mol^{-1} and $\theta_P = -66.7$ K, indicates that the dominant exchanges were similar to **I** and **II**, antiferromagnetic. The large Weiss constant, along with the high ordering

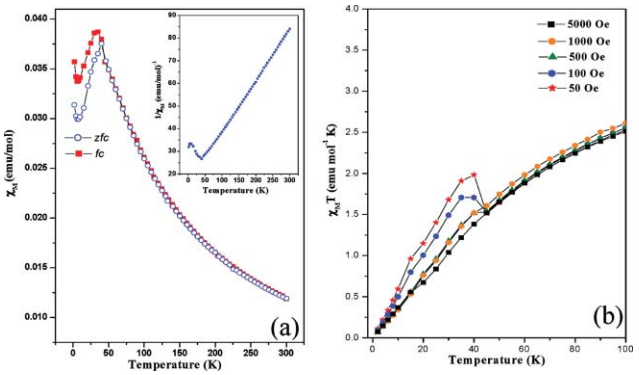

Fig. 3 (a) The thermal variation of the molar susceptibility (χ_M) for **III** under FC and ZFC conditions (H = 1000 Oe). Inset shows the thermal variation of the inverse molar susceptibility ($1/\chi_M$) (ZFC); (b) temperature dependence of the field-cooled $\chi_M T$ at various magnetic fields for **III**.

temperature, indicates that there is a good overlap between the metal and the oxygen orbitals, leading to strengthened super-exchange interactions. The field-cooled $\chi_M T$ *vs.* T curve at different applied dc fields clearly shows the onset of spontaneous magnetization below 42 K, along with an increase in $\chi_M T$ values as the applied field decreases, indicating a canted antiferromagnetic behavior (Fig. 3b). The difference between the field cooled (FC) and the zero-field-cooled (ZFC) susceptibility values at low temperature indicates that there exists a ferromagnet-like correlation.[8] The abrupt jump of $\chi_M T$ below 42 K and the divergence between the ZFC and FC curves at $T \sim 40$ K suggests a long range ordering in **III** with a T_C around 42 K.[9] AC magnetic susceptibility studies also confirm this observation (see ESI†).

In conclusion, the present study demonstrates the importance of entropic considerations in the formation of MOF compounds. The formation of a fully dehydrated brucite-related structure at higher temperature is noteworthy. Since the reaction temperature has a profound effect on the product phases, other variables such as the reaction time, the pH *etc*., are also likely to show interesting effects, and we are currently pursuing work on this theme.

The authors thank DST and CSIR India, for the award of a research grant and fellowship. SN thanks DST for a RAMANNA Fellowship. DST-IRHPA is thanked for the CCD facility.

Notes and references

‡ A mixture of $Mn(OAc)_2 \cdot 4H_2O$ (0.245 g, 1 mM), 4,4′-oxy bis(benzoic acid) (0.21 g, 1 mM), imidazole (0.068 g, 1 mM) and NaOH (0.08 g, 2 mM) were dissolved in 8 ml of water and heated at different temperature (80–220 °C) for 24 h under autogeneous pressure. Pure phases of the compounds (**I**, **II** and **III**) were obtained at 100, 160 and 220 °C, respectively. Pale brown colored block-like crystals of **I**, colorless rectangular crystals of **II** and colorless plate-like crystals of **III**, were obtained in high yield (70–80%). The compounds were characterized by IR, TGA and EPR spectroscopic studies. The structures were determined using a Bruker AXS smart Apex CCD diffractometer at 293(2) K. The structures were solved and refined using SHELXL97 present in the WinGx suite of programs (version 1.63.04a).[10] Restraints for the bond distances were used during the refinement to keep the hydrogen atoms bonded with the water molecules/hydroxyl groups. Crystal data for **I**: $[\{Mn(H_2O)_3\}\{C_{12}H_8O(COO)_2\}]\cdot H_2O$, M = 383.19, monoclinic, space group $P2_1/c$ (no. 14), a = 16.902(6), b = 10.506(4), c = 9.062(3) Å, β = 94.524(5)°, V = 1604.2(9) Å^3, Z = 4, ρ_{cal} = 1.578 g cm^{-3}, $\mu(Mo_{k\alpha})$ = 0.868 mm^{-1}, 13544 reflections, 3760 unique (R_{int} = 0.0277), 3302 observed $I > 2\sigma(I)$, R_1 = 0.0511, wR_2 = 0.1180 and GOF = 1.032 for 242 parameters. For **II**: $[\{Mn(H_2O)\}\{C_{12}H_8O(COO)_2\}]$, M = 329.16, monoclinic, space group $P2/c$ (no. 13), a = 14.399(3), b = 6.3226(15), c = 7.3555(18) Å, β = 102.867(4)°, V = 657.03(3) Å^3, Z = 2, ρ_{cal} = 1.664 g cm^{-3}, $\mu(Mo_{k\alpha})$ = 1.030 mm^{-1}, 5530 reflections, 1558 unique (R_{int} = 0.0345), 1269 observed $I > 2\sigma(I)$, R_1 = 0.0524, wR_2 = 0.0868 and GOF = 1.068 for 101 parameters. For **III**: $[\{Mn(OH)\}_2\{C_{12}H_8O(COO)_2\}]$, M = 400.1, orthorhombic, space group *Pnca* (non-standard setting, no. 60), a = 29.135(8), b = 7.461(2), c = 6.1111(17) Å, V = 1328.4(6) Å^3, Z = 4, ρ_{cal} = 2.001 g cm^{-3}, $\mu(Mo_{k\alpha})$ = 1.938 mm^{-1}, 10371 reflections, 1582 unique (R_{int} = 0.0687), 1227 observed $I > 2\sigma(I)$, R_1 = 0.0892, wR_2 = 0.1321 and GOF = 1.224 for 109 parameters. CCDC: 648374, 648375 and 637649 for **I**, **II** and **III**. For crystallographic data in CIF format see DOI: 10.1039/b708060c

1 (*a*) A. K. Cheetham, C. N. R. Rao and R. K. Feller, *Chem. Commun.*, 2006, 4780; (*b*) D. Maspoch, D. Ruiz-Molina and J. Vaciana, *Chem. Soc. Rev.*, 2007, **36**, 770.

2 P. M. Foster, A. R. Burbank, C. Livage, G. Ferey and A. K. Cheetham, *Chem. Commun.*, 2004, 368.

3 Q. Gao, N. Guillou, M. Nogues, A. K. Cheetham and G. Ferey, *Chem. Mater.*, 1999, **11**, 2937.

4 M. L. Tong, S. Kitagawa, H. C. Chang and M. Ohba, *Chem. Commun.*, 2004, 418.

5 (*a*) M. Kondo, Y. Irie, Y. Shimizu, M. Miyazawa, H. Kawaguchi, A. Nakamura, T. Naito, K. Maeda and F. Uchida, *Inorg. Chem.*, 2004, **43**, 6139; (*b*) M. L. Hu, P. Gao and S. W. Ng, *Acta Crystallogr., Sect. C: Cryst. Struct. Commun.*, 2002, **58**, m323.

6 (*a*) S. M. Humphery and P. T. Wood, *J. Am. Chem. Soc.*, 2004, **126**, 13236; (*b*) Y. Z. Zheng, M. L. Tong, W. X. Zhang and X. M. Chen, *Chem. Commun.*, 2006, 165.

7 M. Dan and C. N. R. Rao, *Angew. Chem., Int. Ed.*, 2006, **45**, 281, and references therein.

8 B. Bazan, J. L. Mesa, J. L. Pizarro, J. R. Fernandez, J. S. Marcos, A. Roing, E. Molins, M. I. Arriortua and T. Rojo, *Chem. Mater.*, 2004, **16**, 5249.

9 S. M. Humphery, A. Alberola, C. J. G. Garcia and P. T. Wood, *Chem. Commun.*, 2006, 1607.

10 (*a*) G. M. Sheldrick, *SHELX-97 Program for crystal structure solution and refinement*, University of Göttingen, Germany, 1997; (*b*) J. L. Farrugia, WinGx suite for small-molecule single crystal crystallography, *J. Appl. Crystallogr.*, 1999, **32**, 837.